

Novel sol-gel synthesis of N-doped TiO₂ hollow spheres with high photocatalytic activity under visible light

Min Qiao · Qiang Chen · Shishan Wu ·
Jian Shen

Received: 29 January 2010/Accepted: 17 May 2010/Published online: 25 May 2010
© Springer Science+Business Media, LLC 2010

Abstract Novel ammonia and triethanolamine assisted sol-gel synthesis method was developed to fabricate the N-doped TiO₂ hollow spheres. The prepared hollow spheres were in submicron size and had good morphology and high specific surface area. Polystyrene (PS) latexes in size of 470 nm were used as the templates to fabricate PS/TiO₂ core–shell spheres. Here ammonia and triethanolamine was first employed together to control the sol–gel process. The N-doped TiO₂ hollow spheres were got after calcinations of the core–shell spheres by using triethanolamine as N source, and the amount of doped N could be easily adjusted by changing the amount of triethanolamine. The hollow spheres had distinct visible light response, and the optical response shifted more to the visible region as the amount of doped N increases. The photodegradation of methylene blue expressed the high photocatalytic activity of the N-doped TiO₂ hollow spheres under visible light.

Keywords Titania · Hollow sphere · Nitrogen doping · Ammonia · Triethanolamine · Photocatalytic activity

M. Qiao · Q. Chen (✉) · S. Wu (✉) · J. Shen
Department of Polymer Science and Engineering, School of
Chemistry and Chemical Engineering, Nanjing University,
210093 Nanjing, China
e-mail: chem100@nju.edu.cn

S. Wu
e-mail: shishanwu@yahoo.com.cn

Q. Chen
High-Tech Research Institute of Nanjing University,
213164 Changzhou, China

J. Shen
College of Chemistry and Environment Science, Nanjing
Normal University, 210097, Nanjing, People's Republic of
China

1 Introduction

Inorganic hollow particles have recently been the subject of extensive research in chemistry and materials science [1, 2]. In this family, the hollow TiO₂ spheres have attracted considerable interest owing to their applications in catalysis, photochemical solar cells, controlled release, chemical sensors and so on [3–9]. The hollow TiO₂ spheres were easily got after removing the polymer core of PS/TiO₂ core–shell spheres. There were two main ways to remove the core: calcinations [10–13] and dissolving by organic solvent [14, 15]. The PS/TiO₂ core–shell spheres were prepared in two main approaches: layer-by-layer self-assembly [16] and sol–gel nanocoating [17–24]. The sol–gel nanocoating was widely used due to its simplicity and high efficiency. But the TiO₂ shells obtained in the sol–gel nanocoating were amorphous, and they could transform from amorphism to anatase or rutile after calcining at different temperature. Anatase or rutile TiO₂ was extensively investigated because of its notable functions for photocatalysis and photoelectron transfer [25–30]. However, the widespread technological uses of TiO₂ were impaired by its wide band gap, which required ultraviolet (UV) irradiation for photocatalytic activation. Because UV light accounts for only a small fraction (5%) of the Sun's energy compared with the visible light (45%), any shift in the optical response of TiO₂ from the UV to the visible spectral range would have a profound positive effect on the photocatalytic efficiency of this material [31]. The widely used approaches that shifted the optical response of TiO₂ from the UV to the visible spectral range were carried out by dye sensitization, metal ion doping, nonmetal doping, etc. [32–41]. Among those, N doping was the most widely used method because it produced p state localization just above the valence band maxima of TiO₂. This greatly

reduced the overall band gap energy of TiO_2 , which led to the red shift of its optical response [41]. Although the N-doped anatase or rutile TiO_2 materials were widely reported, the N-doped anatase TiO_2 hollow spheres with good morphology were rarely reported.

It was well-known that the hydrolysis and condensation of titania precursors was too fast to control [42–44]. So the reagents which acted as inhibitors to slow down the rate of hydrolysis and condensation of titania precursors were needed. Inorganic acids (e.g., nitride acid [24], hydrochloric acid [25]) and organic complexing agents (e.g., acetyl acetone [45], glacial acetic acid [46]) were widely used as inhibitors. But it was hard to use a single agent to control the sol–gel process of titania precursors in various conditions, so here we first employed ammonia and triethanolamine to control the sol–gel process synergistically. Here the active hydroxyl of triethanolamine could induce the transesterification of tetrabutyl titanate to form triethanolamine modified tetrabutyl titanate as illustrated in Fig. 1, which restrained the hydrolysis and condensation of titania precursors [47]. Then the modified tetrabutyl titanate could be dissociated by the more active ammonia, and then the ammonia-catalyzed sol–gel process took place to generate the titania sols. Simonsen et al. [48] investigated the influence of pH on titania sol–gel systems. They found that the TiO_2 particles prepared at alkaline conditions showed the primary particle size of around 3 nm and these primary particles aggregated to form larger secondary particles, and high specific surface area could be achieved for particles synthesized under alkaline conditions independent of the titanium alkoxide used due to the porosity of the secondary particles. Sogimoto et al. [42] also investigated the role of ammonia in the sol–gel formation of TiO_2 spheres. They found that the TiO_2 spheres with smooth surface and high monodispersion could be obtained at appropriate amount of ammonia. Based on above, we achieved to use the assistance of ammonia and

triethanolamine to fabricate N-doped TiO_2 hollow spheres with good morphology and high specific surface area.

On the whole, the facile method developed in this work to fabricate the N-doped anatase TiO_2 hollow spheres involved these novelties and significances below: (1) Ammonia and triethanolamine were first employed here to control the sol–gel process synergistically. The morphology of the core–shell spheres could be easily controlled by changing the amount of ammonia and triethanolamine. (2) Triethanolamine acted also as the nitrogen resource, which was first reported in the fabrication of N-doped TiO_2 hollow spheres. Especially, the amount of doped N can be easily controlled by changing the amount of triethanolamine added. (3) The prepared N-doped TiO_2 hollow spheres were monodisperse with good morphology and high specific surface area. (4) The N-doped TiO_2 hollow spheres had good visible light response and presented high photocatalytic activity under visible light. So the ammonia and triethanolamine assisted sol–gel synthesis reported here was considered as a facile method to prepared N-doped TiO_2 hollow spheres.

2 Materials and methods

2.1 Materials

Styrene (St), triethanolamine and methylene blue were purchased from Shanghai Chemical Reagent Co. (China). Styrene was treated with 10 wt% NaOH aqueous solution to remove the inhibitor and distilled under reduced pressure prior to polymerization. Absolute ethanol, tetrabutyl titanate (TBT), and ammonia solution (25 wt%) were purchased from Nanjing Chemical Reagent Co. (China). Anatase TiO_2 nanoparticles (99%) with the diameter of 25 nm (denoted as TN25) was purchased from Acros (Belgium). Potassium persulfate (KPS) was purchased from Tianjin Chemical Reagent Co. (China) and purified by recrystallization from water. Other reagents of analytical grade were utilized without further purification. Deionized water was applied for all polymerization and treatment processes.

2.2 Methods

2.2.1 Preparation of PS latexes

The monodisperse PS particles in the size of 470 nm were prepared by emulsifier-free emulsion polymerization as follows: 10.0 g of styrene and 90.0 g of H_2O were charged into a 250 mL fourneck flask equipped with a mechanical stirrer, a thermometer with a temperature controller, a N_2 inlet, a Graham condenser, and a heating mantle. The

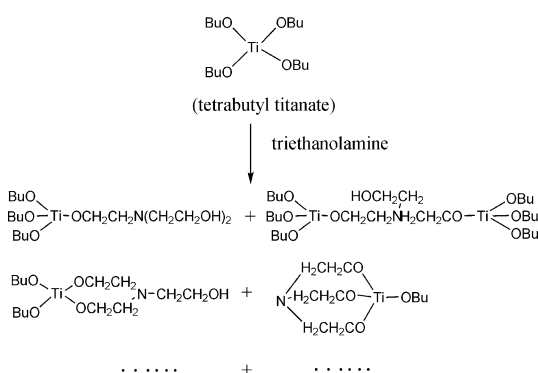


Fig. 1 The schematic illustration of the action of triethanolamine and tetrabutyl titanate

solution was stirred and deoxygenated by bubbling N₂ at room temperature for 20 min. Then, the mixture was slowly heated to 70 °C, followed by addition of an aqueous solution containing 0.1 g of KPS dissolved in 10.0 g of H₂O, and the reaction was carried out at 70 °C for 12 h.

2.2.2 Fabrication of PS/TiO₂ core–shell spheres and N-doped TiO₂ hollow spheres

The PS latexes were reacted with triethanolamine—modified TBT in a solution of ammonia in ethanol to yield PS/TiO₂ core–shell spheres. In a typical procedure: 35 mmol of ammonia and 5.00 g of the PS emulsion (containing ~0.40 g of PS particles) were added into 100 mL of ethanol under stirring, and the mixture was kept at 50 °C for 10 min. Then 4 mL of ethanol solution containing 5 mmol of TBT and 2 mmol of triethanolamine was added dropwise to the suspension under stirring at 50 °C at a rate of 2 mL/h using a syringe pump. The reaction mixture was stirred at 50 °C for an additional 4 h after dripping. The obtained core–shell spheres were separated from the reaction medium by centrifuging, washed several times with ethanol, and then redispersed in ethanol. The core–shell spheres were placed in a furnace, and heated to 500 °C at a rate of 10 °C/min. After holding at 500 °C for 1 h, the sample was cooled down to room temperature at a rate of 20 °C/min. Finally the N-doped anatase TiO₂ hollow spheres were obtained.

2.2.3 The photodegradation of methylene blue

To evaluate the photocatalytic activity of the prepared N-doped TiO₂ hollow spheres, 100 mL of aqueous solution containing methylene blue was placed in a glass beaker with 100 mg of samples. The suspension was placed in dark for 20 min to reach the equilibrium of adsorption and desorption, and then was irradiated with white light (using a white light lamp, 24 W, purchased from Philips, the Netherlands). Aliquots of a few millimeters of the aqueous suspension were collected at regular time periods during irradiation and filtered through syringe filters to remove the hollow spheres. The concentration of methylene blue was estimated by spectrophotometric methods at the maximum absorbance wavelength of 665 nm.

2.2.4 Characterization methods

Transmission electron microscopy (TEM) was performed on a Hitachi H-7650 III microscopy (Japan) operating at 80 kV. The dispersions were diluted with ethanol and ultrasonicated for 10 min and then dried onto carbon-

coated copper grids before examination. Scanning electron microscopy (SEM) was also used to observe the morphology of the particles on Hitachi S-4800 (Japan). The specimens were gold-coated prior to examination. Dynamic Light Scattering (DLS) was used to see the size distributions of the particles on a photon correlation spectrometer (Brookhaven BI-200SM, US). X-ray photoelectron spectroscopy (XPS) were obtained on an ESCA Lab MK II (V.G. Scientific Co. Ltd., UK) equipped with a Mg K α radiation source (12 kV and 20 mA at the anode). The take-off angle of the photoelectron was kept at 45°. The binding energy was referenced by setting the C1s hydrocarbon peak to be 285.0 eV. X-ray diffraction (XRD) analysis was performed on a Shimadzu XRD 6000 diffractometer (Japan). The sample was scanned from 10° to 70° at a scan rate of 5°/min using Cu K α ($\lambda = 0.15406$ nm) radiation at 40 kV and 30 mA. Brunauer-Emmett-Teller (BET) analysis was performed on an instrument of Micromeritics ASAP2020 (USA) at 77 K, with samples degassed at 150 °C for 2 h prior to analysis. The pore volume was estimated from the desorption branch of the isotherm using Barrett-Joyner-Halenda (BJH) method. UV–Visible diffuse reflectance spectra (UV–Vis DRS) were performed on a Shimadzu UV-2401 spectrophotometer (Japan) furnished with an integrating sphere using BaSO₄ as reference.

3 Results and discussion

3.1 Synthesis of the core–shell and hollow spheres

Figure 2a demonstrated the image of PS spheres prepared by emulsifier-free emulsion polymerization. It could be seen that the latex particles are in uniform size of 470 nm and the surface was smooth. Figure 2b showed the image of the PS/TiO₂ core–shell spheres prepared in the typical procedure. The surface of the core–shell spheres became a little rough compared with that of the PS spheres owing to the coating of TiO₂, and it was good to see that the PS spheres were coated with uniform TiO₂ shells. The core–shell spheres were in uniform size of 560 nm. Then the corresponding TiO₂ hollow spheres were obtained by calcining the core–shell spheres. Figure 2c demonstrated the image of the hollow spheres. The diameters of hollow TiO₂ spheres were found to be 20% smaller than that of the corresponding core–shell spheres. In some studies similar phenomenon was also observed owing to shrinkage of the ceramic shells [49, 50]. It could be seen that the hollow spheres were monodisperse and had uniform shells. The size distributions of the PS, PS/TiO₂ core–shell spheres and TiO₂ hollow spheres were given in Fig. 3. It was indicated that they were all monodisperse.

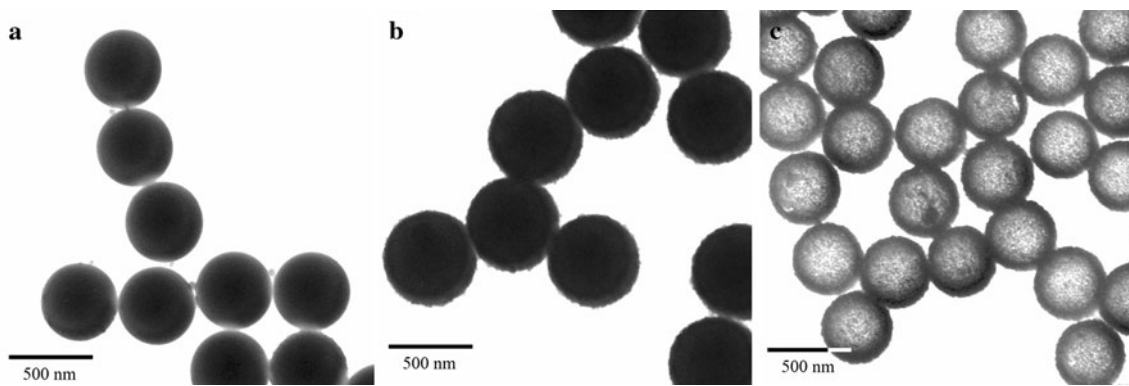


Fig. 2 TEM images of PS spheres (a), PS/TiO₂ core–shell spheres (b) and TiO₂ hollow spheres (c)

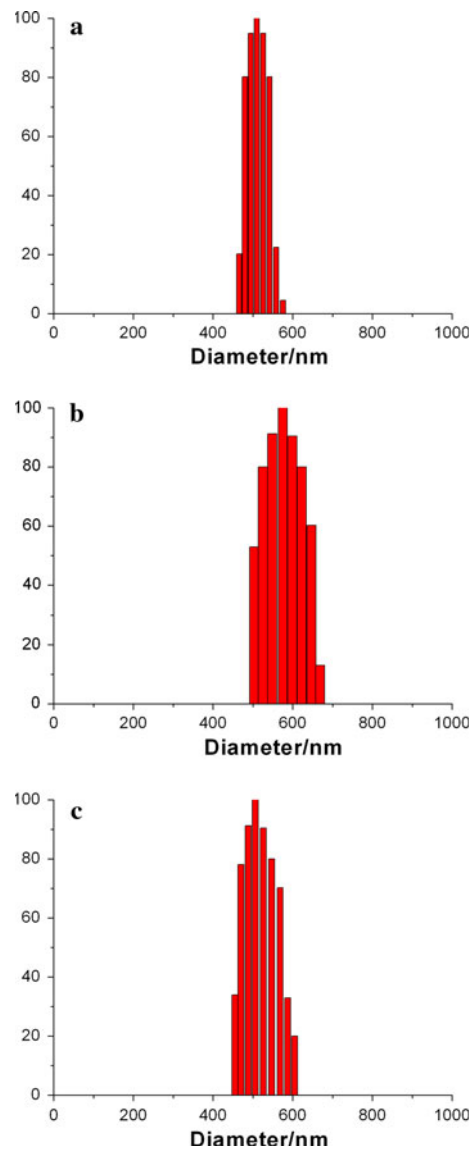


Fig. 3 Size distributions of PS spheres (a), PS/TiO₂ core–shell spheres (b) and TiO₂ hollow spheres (c)

3.2 Effect of ammonia and triethanolamine on the morphology of spheres

Before the coating, TBT reacted with triethanolamine to form triethanolamine-chelated TBT, where triethanolamine acted as a stabilizer of TBT [51]. Then the triethanolamine-chelated TBT was added to the PS suspension in presence of ammonia. The triethanolamine-chelated TBT was first dissociated by the more active ammonia, and then the ammonia-catalyzed hydrolysis and condensation of TBT took place to generate the titania sols. The coating occurred subsequently, even synchronously to form the TiO₂ shells [17, 20]. Ammonia could accelerate hydrolysis and condensation of TBT, and the effect of ammonia on the morphology of the core–shell spheres was shown in Fig. 4. When the amount of ammonia was 14 mmol, the surface of the core–shell spheres was a little rougher compared with that of the spheres prepared in the typical procedure. There were many bigger TiO₂ particles on the surfaces (Fig. 4a). When the amount of ammonia increased to 56 mmol, the surface of the spheres was also rough with many elongated TiO₂ particles on it (Fig. 4c). It indicated that the perfect coating took place when the moderate amount of ammonia was added (Fig. 4b). Furthermore, the effect of the triethanolamine was also investigated. The images of core–shell spheres obtained with different amounts of triethanolamine were shown in Fig. 5. The triethanolamine acted as a stabilizer of TBT, which weakened the hydrolysis and condensation of TBT. When the amount of triethanolamine was 1 mmol, there were some TiO₂ secondary particles or elongated particles on the surface of PS spheres. And when the amount increased to 4 mmol, there were also big TiO₂ nanoparticles on the surface of the spheres. That meant perfect coating took place with the moderate amount of triethanolamine added, which was consistent with the effect of ammonia. We attributed the results above to the synergism of ammonia and triethanolamine. When the

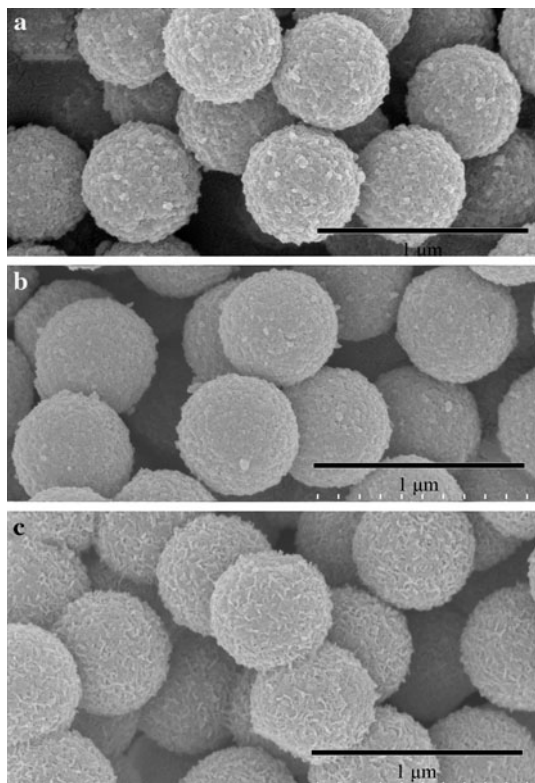


Fig. 4 SEM images of PS/TiO₂ core–shell spheres prepared at different amounts of ammonia: **a** 14 mmol, **b** 35 mmol and **c** 56 mmol

amount of ammonia was low or the amount of triethanolamine was high, ammonia could not dissociate the triethanolamine-chelated TBT totally in short time, so in the system the triethanolamine-chelated TBT could be adsorbed on the generated TiO₂ nanoparticles and prevented them to be captured by PS spheres. When the TiO₂

nanoparticles grew bigger slowly, the triethanolamine-chelated TBT could not provide enough stabilization or be dissociated slowly. Then the big nanoparticles were captured by the PS spheres and led to the surface roughness. On the other hand, when the amount of ammonia was high or the amount of triethanolamine was low, ammonia could dissociate all of the triethanolamine-chelated TBT immediately and accelerated the following hydrolysis and condensation of TBT. The high rate of sol–gel process led to the formation of TiO₂ secondary particles or elongated particles, which also induced the surface roughness of the core–shell spheres. So we can control the morphology of the core–shell spheres just by changing amount of ammonia and triethanolamine relatively. Figure 6 presented the images of PS/TiO₂ core–shell spheres and the corresponding hollow spheres prepared by changing the amount of ammonia and triethanolamine synchronously. It could be seen that all of the core–shell spheres and hollow spheres are in good morphology. So here we considered the synergism of ammonia and triethanolamine as a powerful tool to get desired perfect core–shell spheres and hollow spheres.

3.3 The success of N doping in the hollow spheres

To confirm the success of N doping in the structure of TiO₂, X-ray photoelectron spectroscopy (XPS) was employed to determine the bonding information of Ti and N atoms. Figure 7 showed the XPS spectra of the Ti 2p and N 1s core levels in the hollow spheres. The N 1s core level showed two peaks at 397.0 eV for substitutional N and 399.9 eV for interstitial N [20, 52]. As for the Ti 2p, the typical binding energy of the Ti 2p peak was at 458.0 eV, which was significantly lower than that in P25 powder

Fig. 5 TEM images of PS/TiO₂ core–shell spheres prepared at different amounts of triethanolamine: **a** 1 mmol and **b** 4 mmol

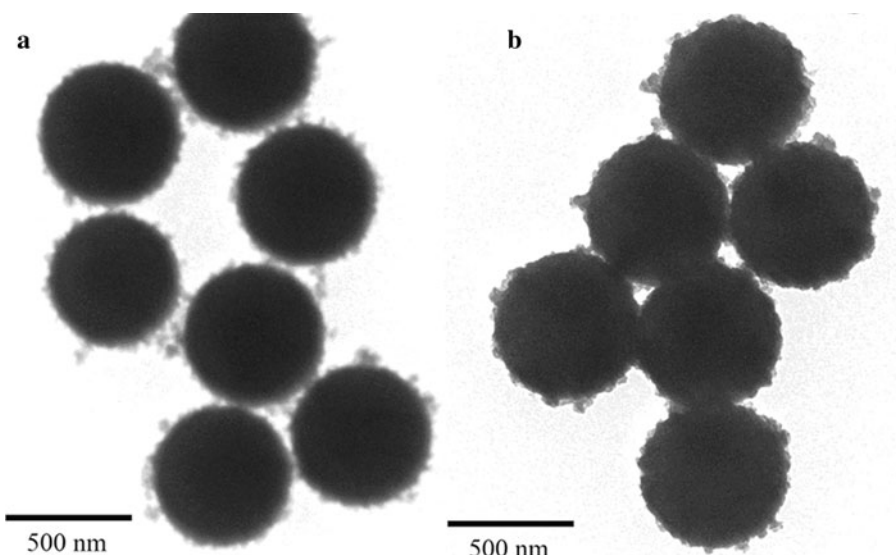
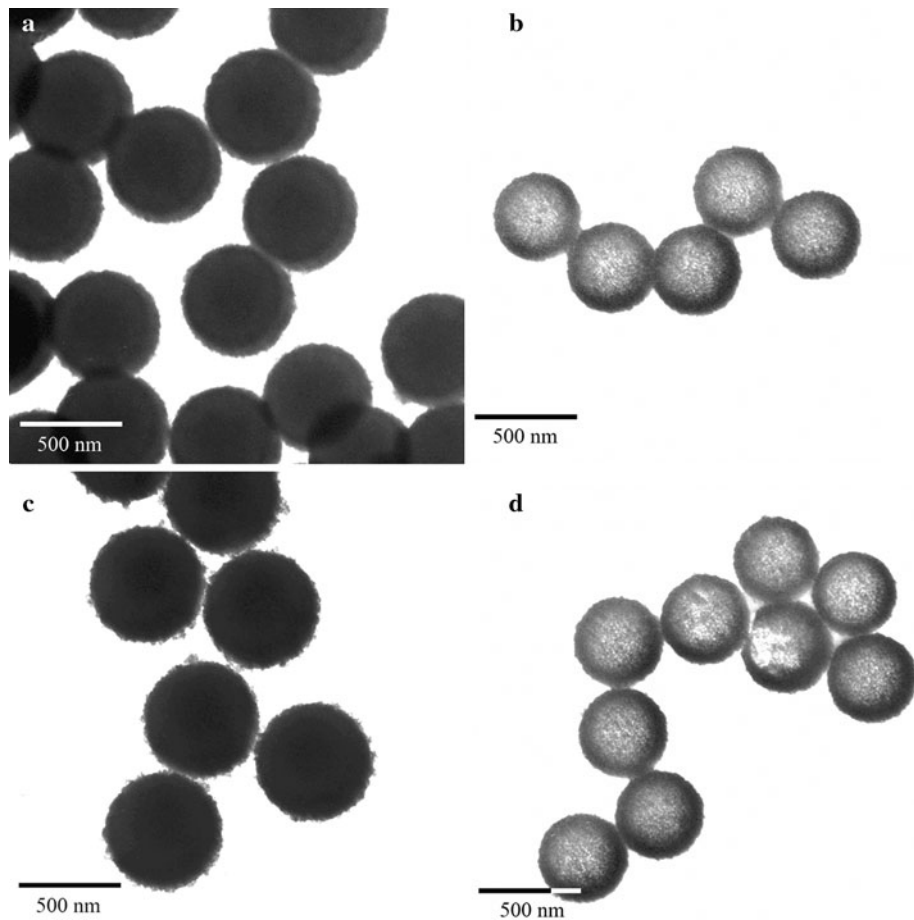


Fig. 6 TEM images of core-shell spheres and hollow spheres prepared at different amounts of ammonia and triethanolamine: **a, b** 14 and 1 mmol; **c, d** 56 and 4 mmol



(459.7 eV) [53], also indicating the N doping. The amount of doped N in the hollow spheres was tested by XPS. The amount of doped N was 0.36, 0.62 and 1.09 atom % when the amount of triethanolamine was 1, 2 and 4 mmol, respectively. It told us that higher amount of triethanolamine resulted in higher amount of doped N in hollow spheres. Because triethanolamine could have covalent bond with Ti [51] and N atoms got introduced due to organic decomposition, some of the N atoms were brought into the crystal lattice instead of being evaporated as gaseous product. At the high boiling point of triethanolamine (~ 360 °C), the transform form amorphism to anatase of TiO_2 progressed slowly [54], which increased the probability of N doping. So we considered triethanolamine as the desired reagent for efficient N doping.

3.4 XRD, BET, and UV–Vis DRS analysis

Figure 8 showed the XRD pattern of the hollow spheres. It could be seen that the TiO_2 shells were transformed from amorphism into anatase phase (JCPDS 21–172) after calcinations. BET analysis was employed to study the textural properties of the hollow spheres. Figure 9 was the BET results of the hollow spheres prepared in typical procedure.

The BET surface area and pore volume of the hollow spheres were calculated to be $70.50 \text{ m}^2/\text{g}$ and $0.19 \text{ cm}^3/\text{g}$, which were larger than the corresponding ones of TN25 (anatase titania nanoparticles in size of 25 nm, BET surface area: $42.50 \text{ m}^2/\text{g}$, pore volume: $0.15 \text{ cm}^3/\text{g}$, tested in the same condition as the hollow spheres). Besides, the hollow spheres had the wide pore size distribution in the range of 3–60 nm. So the hollow spheres obtained in this work were a kind of mesoporous materials with high surface area. The UV–Vis DRS results of the N-doped TiO_2 hollow spheres with different amounts of doped N and TN25 as contrast were shown in Fig. 10. The spectrum of TN25 had only optical response of ultraviolet irradiation (<390 nm), which was similar to the P25 TiO_2 reported [39]. But in the spectra of the N-doped TiO_2 hollow spheres, we could clearly see that there were optical responses in the visible light range (390–600 nm). And the optical response shifted more to the visible region as the amount of doped N increased. So the N doping was effective at improving the visible light response of TiO_2 materials. Based on the discussion above, the N-doped TiO_2 hollow spheres fabricated by us were a kind of mesoporous materials with high surface area and good visible light response.

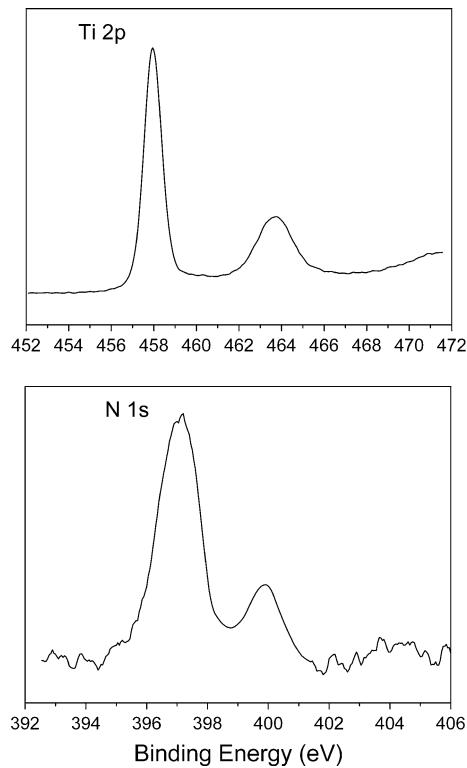


Fig. 7 The XPS spectra of Ti 2p and N 1s core levels in the hollow spheres

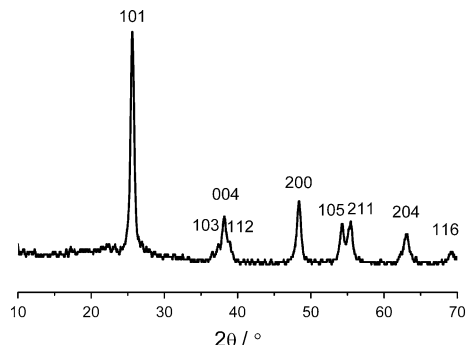


Fig. 8 XRD pattern of hollow spheres prepared in typical procedure

3.5 The photodegradation of methylene blue

To evaluate the photocatalytic activity of the prepared N-doped TiO_2 hollow spheres, the photodegradation of methylene blue (MB) was performed. Figure 11 showed the results of the photodegradation of MB. NTH-1, 2 and 3 was denoted as the N-doped TiO_2 hollow spheres with different amount of doped N: 0.37, 0.62, and 1.09 atom %, respectively. Two blank tests were carried out: the solution of MB without TiO_2 was irradiated for 8 h and only 0.7% of MB degraded; the suspension containing MB and NTH-2 was in dark for 8 h and only 2.2% of MB degraded, which told us that the system had already reached the

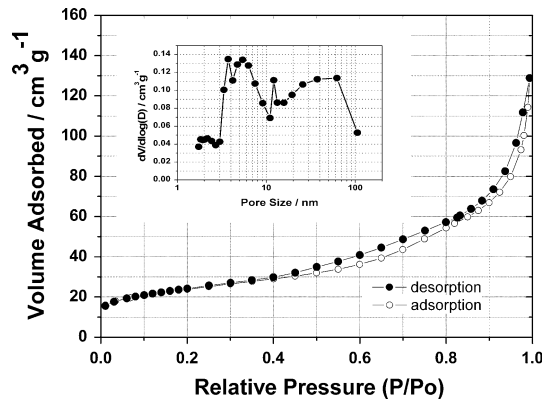


Fig. 9 Nitrogen adsorption–desorption isotherm of the TiO_2 hollow spheres prepared in typical procedure. Insert shows the pore size distribution using the BJH desorption data

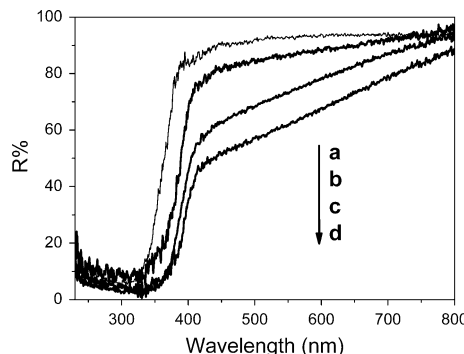


Fig. 10 UV-Vis diffuse reflectance spectra of TN25 (a) and N-doped TiO_2 hollow spheres with different amount of doped N: (b) 0.37, (c) 0.62, (d) 1.09 atom %

equilibrium of adsorption and desorption after 20 min of adsorption and desorption. Based on the two blank tests above, we believed that the results of the photodegradation of MB under white light can provide the direct evidence of the photocatalytic activity of samples under visible light. When using NTH-1, NTH-2 and NTH-3 as the photocatalyst, MB degraded for 74.4, 89.6 and 96.6%, respectively, after irradiated under white light for 8 h. When using TN25 as the photocatalyst, only 13.7% of MB degraded in the same condition. So the N-doped TiO_2 hollow spheres presented excellent photocatalytic activity under visible light, which was due to the N doping [37, 38, 40] and the high surface area [55]. The N-doped TiO_2 hollow spheres were supposed to be a new and significant TiO_2 material with high photocatalytic efficiency.

4 Conclusions

In summary, we had demonstrated a novel ammonia and triethanolamine assisted sol–gel synthesis of monodisperse

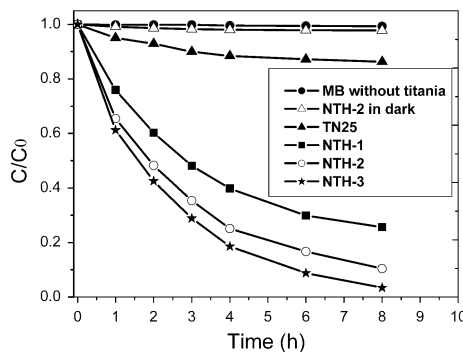


Fig. 11 The photodegradation of methylene blue

N-doped TiO_2 hollow spheres. The morphology of the core–shell could be controlled by the synergism of ammonia and triethanolamine. The N-doped TiO_2 hollow spheres were got after the calcinations of the corresponding core–shell sphere. Triethanolamine was the resource of N elements, and the amount of doped N in the hollow spheres could be easily adjusted by changing the amount of triethanolamine added. The hollow spheres were proven to be a kind of mesoporous materials with high surface area and good visible light response. The N-doped TiO_2 hollow spheres presented excellent photocatalytic activity under visible light, and were supposed to be a new and significant TiO_2 material with high photocatalytic efficiency.

Acknowledgments The authors acknowledge Mr. Kaihe Du (College of Life Science, Nanjing Normal University, China) for his great help in TEM observation, and Mr. Jianxin Wu (University of Science and Technology of China) for his help in XPS testing and analysis.

References

- Hagfeldt A, Grätzel M (1995) Chem Rev 95:49–68
- Zou H, Wu SS, Shen J (2008) Chem Rev 108:3893–3957
- Kim SW, Kim M, Lee WY, Hyeon T (2002) J Am Chem Soc 124:7642–7643
- Caruso F (2000) Chem Eur J 6:413–419
- Zhang M, Gao G, Zhao DC, Li YZ, Liu FQ (2005) J Phys Chem B 109:9411–9415
- Nakamura H, Ishii M, Tsukigase A, Harada M, Nakano H (2005) Langmuir 21:8918–8922
- Li J, Zeng HC (2005) Angew Chem Int Ed 44:4342–4345
- Li YZ, Zhang H, Hu XL, Zhao XJ, Han M (2008) J Phys Chem C 112:14973–14979
- Kondo K, Yoshikawa H, Awaga K, Murayama M, Mori T, Sunada K, Bandow S, Iijima S (2008) Langmuir 24:547–550
- Kabayashi Y, Gu SC, Kondo T, Mine E, Nagao D, Kondo M (2004) J Chem Eng Jpn 37:912–914
- Syoufian A, Inoue Y, Yada M, Nakashima K (2007) Mater Lett 61:1572–1575
- Lia GC, Zhang ZK (2004) Mater Lett 58:2768–2771
- Yang J, Lind JU, Trogler WC (2008) Chem Mater 20:2875–2877
- Imhof A (2001) Langmuir 17:3579–3585
- Agrawal M, Pich A, Zafeiropoulos NE, Stamm M (2008) Colloid Polym Sci 286:593–601
- Caruso RA, Susha A, Caruso F (2001) Chem Mater 13:400–409
- Yang ZZ, Niu ZW, Lu YZ, Hu ZB, Han CC (2003) Angew Chem Int Ed 42:1943–1945
- Zhang K, Zhang XH, Chen HT, Chen X, Zheng LL, Zhang JH, Yang B (2004) Langmuir 20:11312–11314
- Song XF, Gao L (2007) J Phys Chem C 111:8180–8187
- Song XF, Gao L (2007) Langmuir 23:11850–11856
- Li YF, Sun ZQ, Zhang JH, Zhang K, Wang YF, Wang ZH, Chen XL, Zhu SJ, Yang B (2008) J Colloid Interface Sci 325:567–572
- Li HQ, Ha CS, Kim I (2008) Langmuir 24:10552–10556
- Wang P, Chen D, Tang FQ (2006) Langmuir 22:4832–4835
- Guo HX, Zhao XP, Ning GH, Liu GQ (2003) Langmuir 19:4884–4888
- Li YZ, Kunitake T, Fujikawa S (2006) J Phys Chem B 110:13000–13004
- Stone VF, Davis RJ (1998) Chem Mater 10:1468–1474
- Stein A (2003) Adv Mater 15:763–775
- Shechukin DG, Caruso RA (2004) Chem Mater 16:2287–2292
- Yang P, Zhao D, Margolese DI, Chmelka BF, Stucky GD (1998) Nature 396:152–155
- Shibata H, Ogura T, Mukai T, Ohkubo T, Sakai H, Abe M (2005) J Am Chem Soc 127:16396–16397
- Im JS, Yun SM, Lee YS (2009) J Colloid Interface Sci 336:183–188
- Choi W, Termin A, Hoffmann M (1994) J Phys Chem 98:13669–13679
- Asahi R, Morikawa T, Ohwaki T, Aoki K, Taga Y (2001) Science 293:269–271
- Sato S (1986) Chem Phys Lett 123:126–128
- Irie H, Watanabe Y, Hashimoto K (2003) J Phys Chem B 107:5483–5486
- Li D, Haneda H, Hishita S, Ohashi N, Labhsetwar NK (2005) J Fluor Chem 126:69–77
- Ao YH, Xu JJ, Fu DG, Yuan CW (2009) Microporous Mesoporous Mater 118:382–386
- Chi B, Zhao L, Jin T (2007) J Phys Chem C 111:6189–6193
- Estruga M, Domingo C, Domènech X, Ayllón JH (2009) Nanotechnology 20:125604–125611
- Joshi MM, Labhsetwar NK, Mangrulkar PA, Tijare SN, Kamble SP, Rayalu SS (2009) Appl Catal A Gen 357:26–33
- Asahi R, Morikawa T (2007) Chem Phys 339:57–63
- Sugimoto T, Kojima T (2008) J Phys Chem C 112:18760–18771
- Sugimoto T, Kojima T (2008) J Phys Chem C 112:18437–18444
- Sugimoto T, Kojima T (2008) J Phys Chem C 112:18445–18454
- Guo LL, Gao G, Liu ML, Liu FQ (2008) Mater Chem Phys 111:322–325
- Zhou J, Chen M, Qiao XG, Wu LM (2006) Langmuir 22:10175–10179
- Bardley DC, Mehrotra RC, Gaur DP (1986) Metal alkoxides. Academic Press, UK, pp 236–242
- Simonsen ME, Søggard EG (2010) J Sol-Gel Sci Technol 53:485–497
- Cheng XJ, Chen M, Wu LM, Gu GX (2006) Langmuir 22:3858–3863
- Wang D, Caruso F (2002) Chem Mater 14:1909–1913
- Bockmeyer M, Löbmann P (2008) J Sol-Gel Sci Technol 45:251–259
- Saha NC, Tompkins HG (1992) J Appl Phys 72:3072–3079
- Sathish M, Viswanathan B, Viswanath RP, Gopinath CS (2005) Chem Mater 17:6349–6354
- Li YX, Xie CF, Peng SQ, Lu GX, Li SB (2008) J Mol Catal A Chem 282:117–123
- Song CY, Yu WJ, Zhao B, Zhang HL, Tang CJ, Sun KQ, Wu XC, Dong L, Chen Y (2009) Catal Commun 10:650–654